Flavin-Dependent Alkyl Hydroperoxide Reductase from *Salmonella typhimurium*. 2. Cystine Disulfides Involved in Catalysis of Peroxide Reduction†

Leslie B. Poole*

Department of Biochemistry, Wake Forest University Medical Center, Winston-Salem, North Carolina 27157

Received August 11, 1995; Revised Manuscript Received October 16, 1995⊗

ABSTRACT: The two-component alkyl hydroperoxide reductase enzyme system from *Salmonella typhimurium* catalyzes the pyridine nucleotide-dependent reduction of alkyl hydroperoxide and hydrogen peroxide substrates. This system is composed of a flavoenzyme, AhpF, which is related to the disulfide-reducing enzyme thioredoxin reductase, and a smaller protein, AhpC, which lacks a chromophoric cofactor. We have demonstrated that NADH-linked reduction of AhpF under anaerobic conditions converts two cystine disulfide centers to their dithiol forms. The AhpC cystine disulfide center, shown to exist as an intersubunit disulfide bond, is stoichiometrically reducible by NADH in the presence of a catalytic amount of AhpF and can be reoxidized by ethyl hydroperoxide. Disulfide bridges within oxidized AhpF form between Cys129 and Cys132 and between Cys345 and Cys348; the two C-terminal half-cystine residues, Cys476 and Cys489, exist as free thiol groups in oxidized AhpF and play no role in catalysis. Removal of the N-terminal 202-amino acid segment containing the Cys129−Cys132 disulfide center obliterates the ability of AhpF to transfer electrons to 5,5′-dthiobis(2-nitrobenzoic acid) (DTNB) and AhpC. NADH added anaerobically to AhpF causes spectral changes consistent with preferential reduction of both disulfides relative to flavin reduction; the reduction potentials of the disulfide centers are thus appropriately poised for electron transfer from NADH and flavin to disulfide-containing substrates (AhpC or DTNB), and ultimately to peroxides from AhpC. Blue, neutral flavin semiquinone is also generated in high yields during reductive titrations (91% yield during dithionite titrations), although the relatively slow formation of this species indicates its catalytic incompetence. A long wavelength absorbance band beyond 900 nm attributable to an $FADH_2 \rightarrow NAD^+$ charge transfer interaction is generated during NADH, but not dithionite, titrations and may be indicative of a species directly involved in the catalytic cycle. A catalytic mechanism including the transient formation of cysteine sulfenic acid within AhpC is proposed.

The alkyl hydroperoxide reductase (AhpR)[1] enzyme system of *Salmonella typhimurium* has been identified as an antioxidant system capable of reducing, and thereby detoxifying, organic hydroperoxides and hydrogen peroxide in a pyridine nucleotide-dependent manner (Jacobson et al., 1989; Niimura et al., 1995; Poole & Ellis 1996; Storz et al., 1989). Analyses of each of the system's two purified protein components, AhpF and AhpC, have recently been facilitated by the availability of large quantities of pure recombinant proteins (Poole & Ellis, 1996); these recombinant proteins isolated from *Escherichia coli* are fully active and are indistinguishable from AhpF and AhpC purified from *S. typhimurium*.

Catalytic roles for each AhpR protein in the overall reaction have been suggested to follow the same general pattern as the thioredoxin reductase (TrR)/thioredoxin (Tr) system (Chae et al., 1994b; Jacobson et al., 1989; Poole, 1994; Tartaglia et al., 1990). In this proposed scheme, AhpF transfers electrons from reduced pyridine nucleotides to AhpC *via* the flavin and direct dithiol−disulfide interchange, followed by transfer of electrons from the dithiol center of AhpC to the hydroperoxide substrate. Considerable evidence now strongly supports this general scheme. AhpF efficiently catalyzes electron transfer from NADH to at least two different disulfide-containing acceptors, DTNB and AhpC (Poole & Ellis, 1996). Peroxides are very poor substrates for AhpF alone, and the presence of AhpC is required for significant turnover; AhpC in the absence of AhpF does not catalyze NADH-dependent peroxide reduction. Finally, only the reduced forms of AhpF and AhpC, tested independently, are sensitive to modifications by thiol reagents which obliterate peroxidatic activity (Poole & Ellis, 1996). Thus, characterization of these putative cystine disulfide redox centers within each protein and determination of the rates and paths of electron transfer among the redox centers of the entire AhpR system remain.

When the deduced amino acid sequence of AhpF is scanned for putative disulfide redox centers, it is notable that two cysteine pairs, both contained in CXXC motifs, are encoded in the AhpF structural gene and that one of these corresponds in sequence alignments to the known cystine

† This research was supported by NIH Grant GM-50389 and Council for Tobacco Research Scholar Award Number SA006.

* Department of Biochemistry, Wake Forest University Medical Center, Medical Center Boulevard, Winston-Salem, NC 27157. Telephone: 910-716-6711. Fax: 910-716-7671. E-mail: lbp@esv.bgsm.wfu.edu.

⊗ Abstract published in *Advance ACS Abstracts,* December 15, 1995.

[1] Abbreviations AhpR, alkyl hydroperoxide reductase; TrR, thioredoxin reductase; Tr, thioredoxin; TSA, thiol-specific antioxidant protein; DTNB, 5,5′-dithiobis(2-nitrobenzoic acid); TNB, 2-nitro-5-thiobenzoate; NTSB, 2-nitro-5-thiosulfobenzoate; EDTA, ethylenediaminetetraacetic acid; EGTA, GuHCl, guanidine hydrochloride; DTT, dithiothreitol; HPLC, high-performance liquid chromatography; SDS, sodium dodecyl sulfate; $AhpF_{ox}$ and $AhpC_{ox}$, oxidized AhpF and AhpC proteins; $AhpF_{red}$, reduced AhpF [not specifying which redox center(s) is/are reduced]; $AhpC_{red}$, reduced AhpC.

0006-2960/96/0435-65$12.00/0

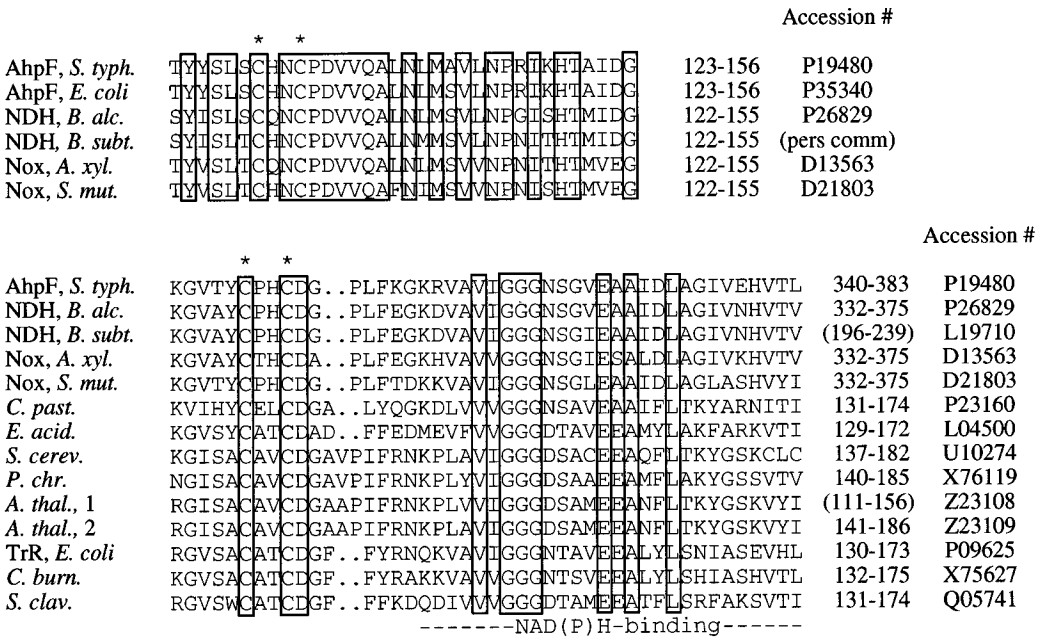

FIGURE 1: Multiple sequence alignments of regions of interest within AhpF and its homologues. Two regions surrounding putative active-site disulfide-forming half-cystine residues are shown; the locations of the regions shown are indicated to the right of the sequence (values in parentheses refer to locations based on sequences which are incomplete at the 5′ end of the structural gene). Accession numbers for the sequences in the DNA and protein data bases are also shown; the *Bacillus subtilis* sequence shown in the top panel was communicated to us by L. Chen and J. D. Helmann. Abbreviations for the organisms denote *Salmonella typhimurium*, *Escherichia coli*, *Bacillus alcalophilus*, *Bacillus subtilis*, *Amphibacillus xylanus*, *Streptococcus mutans*, *Clostridium pasteurianum*, *Eubacterium acidaminophilum*, *Saccharomyces cerevisiae*, *Penicillium chrysogenum*, *Arabidopsis thaliana*, *Coxiella burnetii*, and *Streptomyces clavuligerus*.

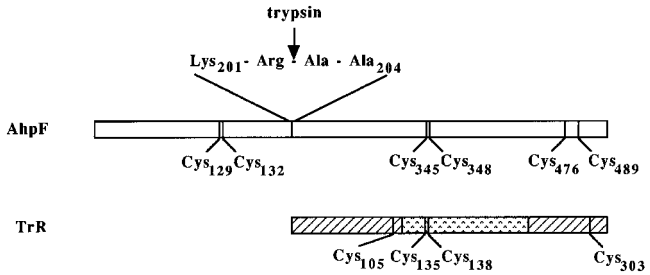

FIGURE 2: Relative locations and alignments of cysteinyl residues within AhpF and TrR. In addition to cysteinyl residue locations and the site of limited tryptic cleavage in AhpF, functional domains determined from the known structure of TrR are shown (hatched regions indicate the noncontiguous FAD binding domain, and the stippled region shows the NADPH binding domain; Kuriyan et al., 1992).

redox center present in TrR (Figure 1; Chae et al., 1994b; Poole, 1994; Tartaglia et al., 1990). Two more cysteinyl residues are located near the C-terminus and are separated by 12 amino acids in the sequence (Figure 2; Tartaglia et al., 1990). In other bacterial flavoproteins identified as close homologues to *S. typhimurium* AhpF (Chae et al., 1994b), all four cysteinyl residues corresponding to the two CXXC motifs of AhpF are absolutely conserved (Figure 1; 55−97% identity among all five homologues shown in the top panel). This is not true for the C-terminal cysteinyl residues of AhpF, which may therefore correspond to the two free thiol groups detected in the oxidized protein (Jacobson et al., 1989). TrR, a more distant homologue of AhpF (35% identity between TrR and codons 215−514 of AhpF), does not have the N-terminal CXXC motif; sequence alignments show that AhpF and its close homologues have approximately 200-amino acid extensions at their N-termini which have no counterpart in the smaller TrR protein (Chae et al., 1994b; Poole, 1994; Tartaglia et al., 1990).

The AhpC structural gene has been shown to encode two cysteinyl residues per monomer; these residues were also identified by alkylation of the reduced protein and sequencing of the carboxamidomethylcysteine-containing peptides (Chae et al., 1994b). In oxidized AhpC, these cysteinyl residues form intersubunit disulfide bridges (as shown by the migration of the protein as a dimer on nonreducing SDS−polyacrylamide gels; Poole & Ellis, 1996); this represents an unusual arrangement for active-site disulfide centers expected to be undergoing reversible reduction during catalysis. Cysteine residues in reduced AhpC are readily modified by *N*-ethylmaleimide treatment under nondenaturing conditions; as stated, this modification completely inhibits peroxidatic activity of AhpC (Poole & Ellis, 1996).

When the possible role of AhpC cysteine residues in peroxide reduction is considered, it is important to recognize that chemical precedent for the involvement of reduced cysteinyl or selenocysteinyl residues in the direct reduction of hydroperoxide substrates has been established for two other heme-independent peroxidases, streptococcal NADH peroxidase (Poole & Claiborne, 1989a,b) and eukaryotic glutathione peroxidase (Epp et al., 1983; Flohé et al., 1972). A homologue of AhpC, the yeast thiol-specific antioxidant protein (TSA), has also recently been shown to require both Cys47 and Cys170, the two cysteinyl residues conserved among most AhpC homologues, for thioredoxin-dependent peroxidatic activity (Chae et al., 1994a).

Studies reported herein have been designed to determine the identity and reactivity of redox-active disulfide centers within both proteins. Cysteinyl residues believed to be present as free thiols in oxidized AhpF have been replaced by alanine residues using site-directed mutagenesis. Spectral characteristics and thiol and disulfide contents of different redox forms of AhpF and AhpC have been described and have been used to develop a proposal for the chemical

mechanism of the alkyl hydroperoxide reductase system.

EXPERIMENTAL PROCEDURES

Materials. Sigma was the supplier of protocatechuic acid and protocatechuate-3,4-dioxygenase. Sodium dithionite was from Fisher. TPCK-treated trypsin was purchased from Worthington Biochemicals. Recombinant AhpF and AhpC proteins were expressed and purified as described in the preceding paper (Poole & Ellis, 1996). The standard buffer used in most experiments was 25 mM potassium phosphate at pH 7.0, with 1 mM EDTA, unless stated otherwise.

Peptide Modification, Preparation, and Sequencing. For exhaustive tryptic digestions of wild type and modified AhpF proteins without pretreatment, 10 nmol of protein in 360 μL of 4 M urea was diluted with buffer to give final concentrations of 2 M urea, 0.2 M ammonium bicarbonate buffer at pH 8.4, and 1 mM $CaCl_2$. Trypsin was added from a stock prepared in 1 mM HCl containing 1 mM $CaCl_2$ to give a final ratio of trypsin to substrate of 1:30 (w/w). Samples were incubated at 37 °C for 24 h, with a second aliquot of trypsin added at 12 h. The digested sample was injected directly onto an HPLC column for peptide separations or frozen at −20 °C for later use.

Pretreated samples for exhaustive tryptic digestions were prepared in 360 μL volumes containing 10 nmol of protein, 4 M urea, 0.25 M Tris-HCl at pH 7.5, and 1 mM EDTA. In some cases, a 100-fold molar excess of DTT over protein was added and incubated at room temperature for 30 min. Pyridylethylation of cysteine residues based on the method of Fullmer was also carried out for some samples (Fullmer, 1984) and involved the addition of 2.6 μL of 4-vinylpyridine (about 2:1 molar excess over DTT thiols) and incubation for 90 min at room temperature, after which the solution was acidified with acetic acid (32.5 μL of acetic acid added, pH <4.0). These samples were dialyzed against 12 L of 10 mM acetic acid, followed by 12 L of deionized water, frozen, and lyophilized. Tryptic digestions were carried out as described above.

HPLC separations were carried out using a Waters HPLC system fitted with a 4.6 × 100 mm AquaPore RP-300 C8 column, using a gradient of acetonitrile containing 0.1% trifluoroacetic acid. Peaks were detected at 215 and 254 nm using a DynaMax UV-DII dual wavelength detector. One peptide, Pep1-D, was rechromatographed using a much shallower gradient for additional purification prior to sequence analysis. Amino acid sequence analyses were performed in the Protein Analysis Core Laboratory of the Cancer Center of Wake Forest University, supported in part by NIH Grants CA-12197 and RR-04869, as well as by a grant from the North Carolina Biotechnology Center.

Preparation and Isolation of the 37 kDa Tryptic Fragment of AhpF. Limited tryptic digestion of native AhpF for large scale preparation of the 37 kDa fragment was carried out by incubation of 17 mg of AhpF with trypsin (1:60 trypsin: AhpF, w/w) in 1 mL of a solution containing the same buffer components described above, but lacking urea. This mixture was incubated at 37 °C for 45 min, then chilled on ice, and brought to 4 mM in EGTA. The entire sample was applied to the top of a BioGel A-0.5m column and eluted with standard buffer; fractions were analyzed for purity on SDS−polyacrylamide gels, and the pure 37 kDa fragment was aliquoted and stored at −20 °C for later use. The isolated tryptic fragment of AhpF was submitted for N-terminal sequence analyses following ultrafiltration to decrease the phosphate buffer concentration as described previously (Poole & Ellis, 1996).

Thiol and Disulfide Assays. Assays for free thiol groups within the oxidized proteins were carried out by addition of 4 M GuHCl or 2% SDS and 100 μM DTNB, followed by detection of the TNB produced at 412 nm using the reported extinction coefficient of 14 150 M^{-1} cm^{-1} (Riddles et al., 1979). Corresponding assays of reduced proteins were carried out by addition of 4 M GuHCl and then 100 μM DTNB to anaerobic solutions of the protein(s) to which excess NADH had been added. Protein disulfides were assayed by the spectrophotometric method described by Thannhauser et al. (1984), which employs sulfitolysis of protein disulfides under denaturing conditions (6 M GuHCl in this case) followed by reaction with the sulfite-insensitive thiol reagent NTSB. Care was taken to avoid exposure of reaction mixtures to room light. Disulfide content was calculated from the extent of the NTSB reaction corrected for the contribution from free thiol groups as determined by DTNB assays described above. All disulfide and thiol assays were performed in 0.5−1.0 mL volumes containing sufficient protein to generate A_{412} values between 0.5 and 1.0 (except for oxidized AhpC, which was included at 14 μM).

Mutagenesis and DNA Sequence Comparisons. In order to replace Cys476 and Cys489 of AhpF with Ser or Ala in both positions, mutagenic oligonucleotides of the following sequences were designed: 5′-GACGCCAAAT/GCCGAAAC-CAGC-3′ and 5′-CAGGCGATT/GCCACCACCG-3′ (oligonucleotide synthesis was performed in the DNA Synthesis Core Laboratory of the Cancer Center of Wake Forest University, supported in part by NIH Grant CA-12197). To generate the single-stranded template for mutagenesis, the 3.1 kb *Sal*I-*Msc*I fragment from pAQ27 (Tartaglia et al., 1990) was cloned into the *Sal*I-*Eco*RV sites of pBluescriptII SK+, followed by removal of the 1.4 kb *Xho*I-*Nhe*I fragment to delete the AhpC structural gene. Single-stranded DNA was generated using single-stranded rescue by R408 helper phage from Stratagene (Russel et al., 1986). Mutagenesis was first performed to introduce the Ser and Ala substitutions at Cys489 as recommended using the oligonucleotide-directed *in vitro* mutagenesis kit (version 2.1) from Amersham. Following identification of each desired mutant by sequence analysis, each single-stranded template containing either the Ser or the Ala mutation at codon 489 was prepared as before and used in a second round of mutagenesis to create mutations at codon 476, as well. Following mutagenesis using the Sculptor *in vitro* mutagenesis system from Amersham, sequence analysis permitted identification of the C476,489S and C476,489A mutations (although both mutations, as well as C476A,C489S and C476S,C489A, were generated, only the C476,489A was subcloned into the expression vector for further characterization). The 483 bp *Eag*I-*Sma*I fragment from the pBluescriptII SK(+) vector containing the mutated region of the C476,489A AhpF structural gene was subcloned into the *Eag*I and blunted *Bst*XI sites of pAF1 (Poole & Ellis, 1996) following dephosphorylation of the digested vector fragment (the *Bst*XI site was blunt ended by a 10 min treatment with T4 DNA polymerase at 37 °C followed by another 10 min incubation after addition of dNTPs). Confirmation that the correct

Table 1: Characteristics of Wild Type and Modified Forms of AhpF

characteristic	AhpF (wild type)	AhpF/C476,489A	tryptic fragment (wild type)	tryptic fragment (C476,489A)
free thiols (DTNB)[a,b]	2.01	0.06	1.80	0.07
disulfides (NTSB)[a,c]	2.04	1.83	0.96	0.95
free thiols, protein reduced with excess NADH (DTNB)[a]	6.01	3.46	3.60	1.61
ϵ_{450} of bound FAD (M^{-1} cm^{-1})	12900	13200	12700	12700
A_{280}/A_{450}	5.6	5.3	4.6	4.5
FAD content (FAD/subunit)	0.92	1.09	1.12	1.07
peroxide reductase activity (min^{-1})[d,e]	1500	1660	16	15
transhydrogenase activity (min^{-1})[d]	2730	2320	2860	2390
DTNB reductase activity[d,f]				
standard assay conditions (min^{-1})	1110	995	35	35
steady state kinetic analysis				
$V_{max,app}$ (min^{-1})	882	900	ND[g]	ND
$K_{m,app}$ for NADH (μM)	0.58	1.07	ND	ND

[a] Expressed per subunit; values shown for thiol and disulfide contents are an average of at least two experiments. [b] Assayed under conditions where 2 SH/mol would give an A_{412} of at least 0.4. [c] NTSB reaction corrected for free thiols (DTNB reaction, top row). [d] Activities are expressed relative to moles of FAD determined at 450 nm; values shown are an average of at least three measurements. [e] AhpF samples assayed in the presence of 5 nmol of recombinant AhpC. [f] [DTNB] = 500 μM; kinetic parameters were determined using the program ENZFITTER. [g] ND = not determined.

mutations were present and that the rest of the subcloned DNA fragment sequence was correct was obtained by DNA sequence analysis through the entire region between and around the restriction sites used.

Programs used in searching for homologues to the genes of interest (FASTP, TFASTP, and BLAST) and for multiple sequence alignments (PILEUP) were run locally on a VAXstation 3100 using the Genetics Computer Group suite of programs and on the Y-MP/832 and C90 machines at the Pittsburgh Supercomputing Center, supported through the NIH Division of Research Resources Cooperative Agreement 1 P41 RR06009-01.

Spectral and Anaerobic Experiments. A Milton Roy Spectronic 3000 diode array spectrophotometer with 0.35 nm resolution was used to collect all absorbance spectra and to carry out all anaerobic absorbance measurements. Aerobic assays monitoring absorbance changes at a single wavelength were carried out using a thermostatted Gilford 220 recording spectrophotometer with a DU monochromator. Assay methods and extinction coefficients were described in the preceding paper (Poole & Ellis, 1996).

Spectrophotometric titrations carried out under anaerobic conditions were conducted using a glass titration cuvette assembly essentially like that described by Williams et al. (1979), with repeated evacuation and nitrogen flushing of solutions over at least 20 min. Dithionite solutions were prepared in standard buffer and standardized by anaerobic titration of a solution of free flavin adenine dinucleotide (FAD). All anaerobic experiments other than dithionite titrations included an oxygen-scrubbing system of 40 μM protocatechuic acid and 0.02 u/mL protocatechuate dioxygenase (Bull & Ballou, 1981). All spectral data were corrected for dilution, which was generally <3%. Unless otherwise indicated, dithionite titrations included a $^1/_{100}$ mol equiv (compared with AhpF) of methyl viologen to promote electron transfer between redox centers within the enzyme (Prongay & Williams, 1992).

RESULTS

Thiol and Disulfide Content of Redox Forms of AhpF and AhpC; Peroxide-Mediated Oxidation of Reduced AhpC. In studies designed to assess the conversion of disulfide bonds to dithiols as a result of pyridine nucleotide-linked reduction, we performed thiol and disulfide assays on different redox forms of each AhpR protein. Our analyses of the oxidized proteins confirmed the thiol content of 2 and 0 for AhpF and AhpC monomers, respectively, as previously reported by Jacobson et al. (1989), and demonstrated by NTSB assay that 2 and 1 disulfide bond(s) per monomer were present in AhpF and AhpC, respectively (Table 1). Analyses by SDS−polyacrylamide gel electrophoresis had already shown that AhpC, but not AhpF, possesses intersubunit disulfide bonds and migrates as a dimer under nonreducing conditions (Poole & Ellis, 1996).

Scheme 1[a]

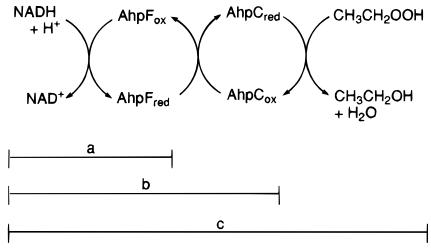

[a] Parts a−c refer to the individual experiments described in the text. Thiol contents after addition of excess NADH were 6 SH/subunit (from 2 SH/subunit in oxidized protein) for AhpF (a), 2 SH/subunit for AhpC (b), and 0 SH/subunit for AhpC after ethyl hydroperoxide treatment (c).

In the first step of the proposed mechanism, AhpF is reduced by pyridine nucleotides [NADH is a better reductant than NADPH (Poole & Ellis, 1996)]; electron transfer is expected to proceed first to the bound FAD and then to one or both cystine disulfide centers in the protein (Scheme 1, part a). We have found that both disulfide centers of AhpF are, in fact, reduced to dithiols in the protein reduced anaerobically with excess NADH (Table 1). This result is in reasonable agreement with values reported by Jacobson et al. (1989) for DTT- and NADPH-reduced AhpF, although their assays, carried out with relatively limited amounts of protein, yielded thiol contents that were a little higher (about 7−8 SH/subunit). Redox forms of AhpF generated during the course of static titrations with NADH can be monitored spectrally; characterization of these partially reduced species is described in a later section.

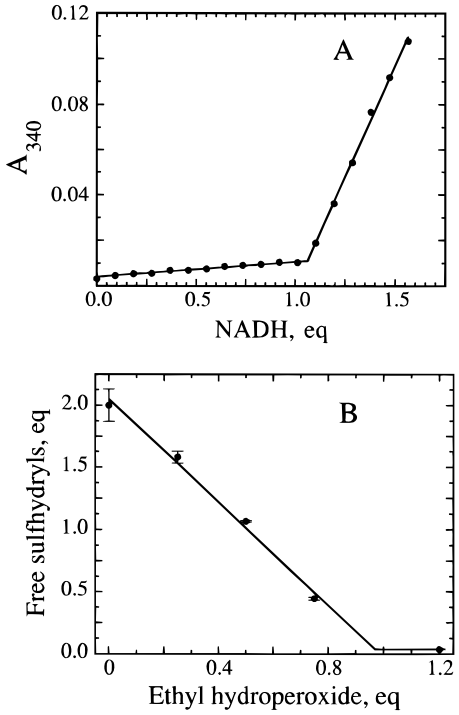

FIGURE 3: Anaerobic NADH titration of AhpC in the presence of the AhpF. AhpC (18.5 nmol) and AhpF (90 pmol) were combined and made anaerobic in 0.6 mL of a solution containing protocatechuate dioxygenase (0.02 u) and protocatechuic acid (20 nmol) to eliminate oxygen, 1 mM EDTA, and 50 mM potassium phosphate at pH 7.0. Spectra were then collected after all changes were complete following each addition of an aliquot of NADH (1.35 mM stock, 1.3 μL per addition) added from a titrating syringe containing the anaerobic solution. (A*)* Absorbance monitored at 340 nm *vs* equivalents of NADH added (relative to AhpC monomer). As shown, 1.07 equiv of NADH was oxidized during the course of this titration; results from six experiments gave an average of 1.19 ± 0.16 NADH/AhpC monomer. (B) Following anaerobic NADH titrations of AhpC as depicted in Panel A and elimination of excess NADH through the AhpF-dependent oxidase activity (the anaerobic cuvette was opened to air and allowed to equilibrate), additions of ethyl hydroperoxide were made prior to spectral assay for thiols with 100 μM DTNB. Shown are the resulting thiol titer values expressed as a function of ethyl hydroperoxide added, each expressed relative to AhpC monomer. Each data point is the average of two or more separate experiments, shown with standard error bars. The overall stoichiometry for ethyl hydroperoxide-linked thiol oxidation was 0.97 equiv of ethyl hydroperoxide per AhpC monomer.

Following the reduction of AhpF by NADH, electrons are proposed to pass from AhpF to AhpC directly through thiol−disulfide interchange between the proteins (Scheme 1, part b). To monitor the reduction of AhpC by the NADH/AhpF system, we prepared an anaerobic solution of AhpC containing $^1/_{200}$ mol equiv of AhpF to mediate electron transfer and monitored the changes in 340 nm absorbance on titration with NADH (AhpF is absolutely required for this electron transfer to occur). Our results verified that two free thiol groups per subunit (1.95 ± 0.14; $N = 8$) were generated within AhpC on oxidation of a stoichiometric amount of NADH (Figure 3A). These thiol groups react readily with DTNB whether or not denaturant is added, demonstrating their accessibility in the reduced protein. Neither aerobically added NADH nor anaerobically added NADPH at a 20-fold excess resulted in the full generation of two free thiol groups per AhpC monomer (both experiments gave ∼1.4 SH/subunit).

This experiment was also extended to assess the reactivity of the nascent thiol groups of reduced AhpC toward hydroperoxide (Scheme 1, part c). Indeed, stoichiometric ethyl hydroperoxide (standardized independently with horseradish peroxidase and *o*-dianisidine) oxidizes the thiol groups of reduced AhpC to regenerate the disulfide bonds of the oxidized protein (Figure 3B). The oxidized AhpC protein which results from ethyl hydroperoxide- or DTNB-dependent oxidation of the thiols within reduced AhpC is identical to the untreated oxidized protein; this was established by detection of 1.06 disulfide bonds per AhpC monomer by NTSB assay, repeated anaerobic titration of the protein with NADH in the presence of AhpF, and the absence of TNB release following DTT treatment of the reisolated, DTNB-oxidized AhpC. These experiments have thus demonstrated that AhpC possesses two redox-active disulfide centers per dimer, involving both Cys46 and Cys165, which are apparently equally capable of reducing hydroperoxides in their dithiol (reduced) forms. These nascent thiols of reduced AhpC are also capable of complete reduction of DTNB to release two TNB anions.

Assignment of the Free Thiol Groups of Oxidized AhpF as Cys476 and Cys489. Experiments described above have demonstrated the presence of two redox-active disulfide centers and two free thiol groups within oxidized AhpF, the latter of which are not likely to play a role in catalysis. In part on the basis of the structural arrangement (Figure 2) and degree of conservation among homologues (Figure 1) of the six half-cystine residues encoded in the AhpF structural gene, the two C-terminal cysteinyl residues were predicted to be the source of the two free thiol groups of oxidized AhpF. In order to clearly assess whether or not these cysteinyl residues play any role in catalysis by AhpF, Cys476 and Cys489 were both replaced by alanine residues to generate the C476,489A mutant of AhpF. As shown in Table 1, replacement of these cysteinyl residues by alanine did not alter catalytic activity (measured as peroxidase, DTNB reductase, oxidase, and transhydrogenase activities) but did delete the two free thiol groups of oxidized AhpF without affecting the two redox-active disulfide centers within the protein. Steady state kinetic parameters using the DTNB reductase assay ([DTNB] = 500 μM) clearly indicated identical $V_{max,app}$ values (∼890 min^{-1}) and very similar $K_{m,app}$ values for NADH (1.07 and 0.58 μM, respectively) for mutant and wild type proteins. Static NADH titrations as described for the wild type protein in a later section also gave identical results for the C476,489A mutant of AhpF.

Identification of Redox-Active Disulfide Centers within AhpF; Requirement of the N-Terminal Domain Containing Cys129 and Cys132 for Electron Transfer to AhpC or DTNB. Although circumstantial evidence was strong that Cys129−Cys132 and Cys345−Cys348 disulfide bonds formed the non-flavin redox centers in AhpF, we set out to definitively address the arrangement of the disulfide bonds in oxidized AhpF. Preliminary studies had shown that limited tryptic digestions of AhpF could be used to generate a 37 kDa tryptic fragment which retained the ability to bind FAD (the size of the fragment was estimated by SDS−polyacrylamide gel electrophoresis). Recognizing the potential utility of this truncated protein in sorting out disulfide centers, we isolated the truncated protein from the much smaller peptides by gel filtration chromatography and submitted the isolated fragment for sequence analysis. Identification of the amino acids in

the first 13 sequencer cycles showed that only one unambiguous sequence was detected and that the N-terminus of the isolated fragment began at Ala203 (Figure 2). Analyses of the thiol and disulfide contents of the truncated protein confirmed that this modified protein retains both free thiol groups but only one of the two redox-active disulfides present in the wild type protein (Table 1). Similarly, tryptic fragment prepared from the C476,489A mutant of AhpF has only one redox-active disulfide and, like the parent mutant protein, does not possess free thiol groups in its oxidized form (Table 1). These results provide strong confirmation that cysteinyl residues within the N-terminal region of AhpF are not covalently linked to those within the other CXXC motif in the oxidized protein (i.e. Cys129−Cys345 or Cys129−Cys348 bonds were not present as shown by the absence of a second sequence for the isolated fragment).

Although the tryptic fragment of AhpF retains bound FAD and is reducible by NADH, removal of the N-terminal region containing Cys129 and Cys132 results in the loss of NADH-dependent peroxidase and DTNB reductase activities (Table 1). The truncated protein does not appear to be significantly altered in structure, as shown by the spectral properties of the bound flavin and by the full retention of NADH-dependent oxidase and transhydrogenase activities relative to the intact AhpF protein (Table 1).

Direct sequence analyses of a disulfide-containing tryptic peptide from AhpF provided the final definitive evidence that Cys129−Cys132 and Cys345−Cys348 were the two redox-active disulfide centers. Comparison of HPLC-generated tryptic maps of untreated and reduced, pyridylethylated AhpF indicated the generation of several new peaks at 254 nm for the pyridylethylated protein (Pep1-PE and Pep2-PE, Figure 4, Panel D) and the concomitant loss of at least one peak from the oxidized AhpF digest (Pep1-D, Figure 4C). Cystine-containing peptides, which possess some 254 nm absorbance, should exhibit changes in mobility and increase dramatically in 254 nm absorbance following reduction and pyridylethylation (Fullmer, 1984). On further HPLC purification of the putative disulfide-containing peptide peak at 46 min (Pep1-D) from the oxidized AhpF digest, reduction and pyridylethylation of a small amount of the peptide shifted the retention time of this peak to 39 min, corresponding to one of the major peaks (Pep1-PE) seen in the reduced, pyridylethylated AhpF digest (Scheme 2; Figure 4D). Similar analyses of the isolated 37 kDa tryptic fragment of AhpF also indicated the presence of this putative disulfide-containing peptide (Figure 4A), although a number of the other peaks were missing. The other major pyridylethylcysteine-containing peptide (Pep2-PE in Figure 4D) was identified as a C-terminal cysteine-containing peptide (Cys476 and/or Cys489) by its absence from the similarly treated C476,489A protein (data not shown). Amino acid sequence analysis of the isolated peptide (Pep1-D) was indeed consistent with the expected sequence surrounding Cys345 and Cys348; results indicated the presence of an internal disulfide bond between these half-cystine residues in the peptide derived from oxidized AhpF (Table 2). We therefore conclude that the two redox-active disulfide centers of AhpF correspond to Cys129−Cys132 and Cys345−Cys348.

Reductive Titrations of the Three Redox Centers within AhpF. As shown in Figure 5, anaerobic titration of recombinant AhpF with NADH leads to the gradual loss of 450 nm absorbance and generation of a strong absorbance band centered at 575−580 nm. This pattern of absorbance changes is readily identified by comparison with such changes in well-characterized flavoproteins which stabilize the blue, neutral form of flavin semiquinone (FADH•; Massey & Palmer, 1966; Zanetti et al., 1968). This species is the same semiquinone form which can be stabilized by TrR, although, unlike TrR, the extent of semiquinone formation in AhpF titrated with the reduced pyridine nucleotide is not affected by room light. Dithionite titrations also lead to formation of the blue, neutral semiquinone species (Figure 6). Spectral changes during the final phase of the dithionite titration indicate full reduction of the flavin (the low level of absorbance around 600 nm is not attributable to methyl viologen, as shown when this reagent is excluded from the mixture). NADH, on the other hand, does not readily reduce the flavin semiquinone (Figure 5A). At 4 equiv/FAD, the 580 nm absorbance is still rising, and AhpF in the presence of a 20-fold molar excess of NADH also appears to retain some semiquinone (in addition to other long wavelength absorbance, see below).

Spectral analyses of the reduced flavin species formed during dithionite titrations allow for the calculation of the extent of semiquinone formation and of extinction coef-

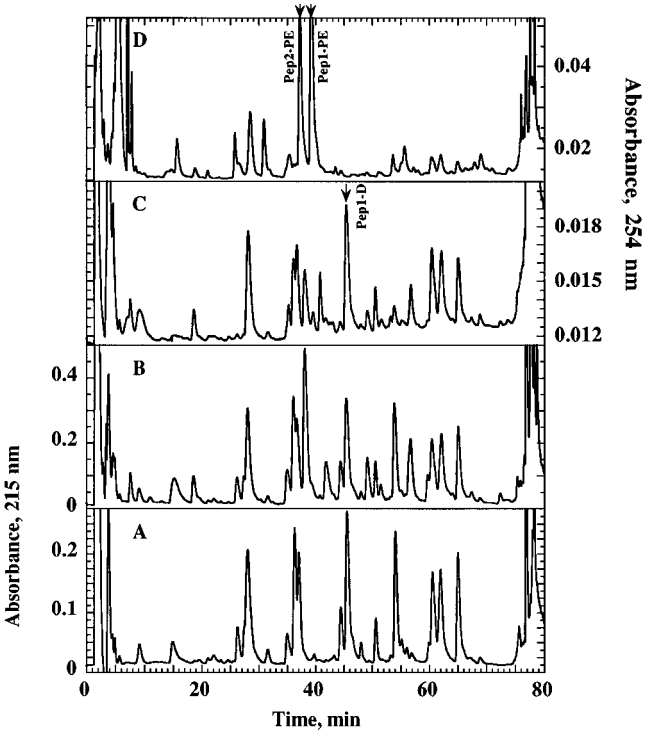

FIGURE 4: HPLC separation of tryptic peptides from oxidized or reduced and pyridylethylated AhpF and its 37 kDa tryptic fragment. Approximately 6 nmol of an exhaustive tryptic digest of AhpF C-terminal tryptic fragment (A), untreated AhpF (B and C), or reduced and pyridylethylated AhpF (D) was applied to an AquaPore RP-300 C8 column. After a 5 min wash with 3.5% acetonitrile in 0.1% trifluoroacetic acid, peptides were eluted with a linear gradient from 3.5 to 28% acetonitrile, in 0.1% trifluoroacetic acid, over 65 min (flow rate of 1 mL/min). A gradient from 28 to 70% acetonitrile in 0.1% trifluoroacetic acid was then applied over 10 min. Peptide elution was monitored at 215 nm (A and B) and 254 nm (C and D).

Scheme 2

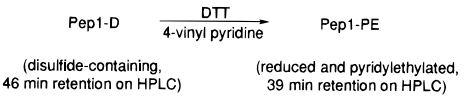

Table 2: Amino Acid Sequence Analysis Of Purified Pep1-D from AhpF

cycle	major peak (pmol)		minor peak (pmol)	
1	Gly	321	–	–
2	Val	359	Gly	13
3	Thr	275	Val	43
4	Tyr	268	Thr	30
5	no peak	–	Tyr	36
6	Pro	135	–	–
7	His	47	Pro	47
8	Xxx[a]	–	His	20
9	Asp	91	Xxx[a]	–
10	Gly	44	Asp[b]	56
11	Pro	20	Gly	26

[a] Peak eluting at 14.7 min, just after Arg (13.5 min) and Tyr (13.9 min); no standard available for identification and quantitation. [b] Although Asp is present in larger amounts than Gly in this cycle, it is listed as the minor peak due to the expectation that its presence is a result of the significant lag from the previous cycle. Yields of amino acids drop off precipitously beginning at cycle 6, and the lag increases, possibly due to the presence of the presumed cystine disulfide bond between residues 5 and 8 and of proline, which may not cleave efficiently.

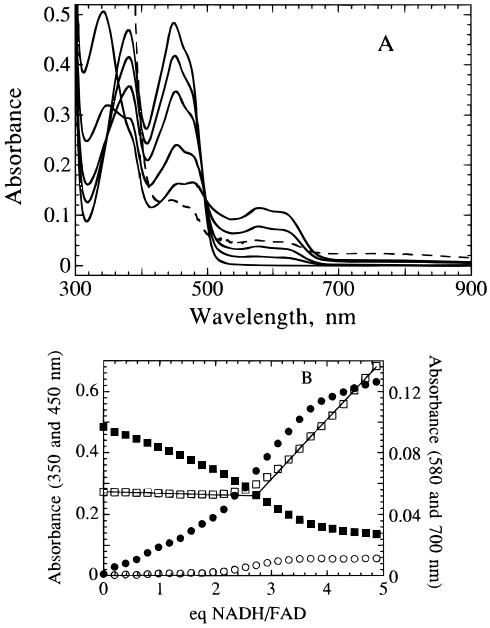

FIGURE 5: Anaerobic NADH titration of AhpF. AhpF (18.5 nmol) in 25 mM potassium phosphate (pH 7.0) containing 1 mM EDTA and the oxygen-scrubbing system (see Figure 3A) in a total volume of 0.5 mL at 25 °C was made anaerobic and titrated with a 2.78 mM anaerobic solution of NADH. Panel A shows spectra (solid lines) obtained after addition of 0, 0.98, 1.95, 2.93, and 3.90 equiv of NADH/FAD, in order of decreasing A_{450} and increasing A_{580}. The dashed line represents the AhpF spectrum obtained in a separate experiment after addition of 20 equiv of NADH/FAD. Panel B depicts the absorbance changes at 350 (open squares), 450 (closed squares), 580 (closed circles), and 700 nm (open circles) *vs* added NADH. Intersection of the linear portions of the 350 nm absorbance changes (near the isosbestic point for FAD and FADH•) indicates oxidation of 2.73 equiv of NADH/FAD.

ficients for the different species formed (Table 3, Figure 6C). A calculated spectrum of the blue, neutral semiquinone (assuming that equal amounts of oxidized and reduced flavin are present at the point of maximal semiquinone and that only one spectral form of semiquinone is observed) is also shown in Figure 6 (dotted spectrum). AhpF is capable of stabilizing an even higher percentage of blue, neutral semiquinone (about 91%) than is TrR (82% yield on

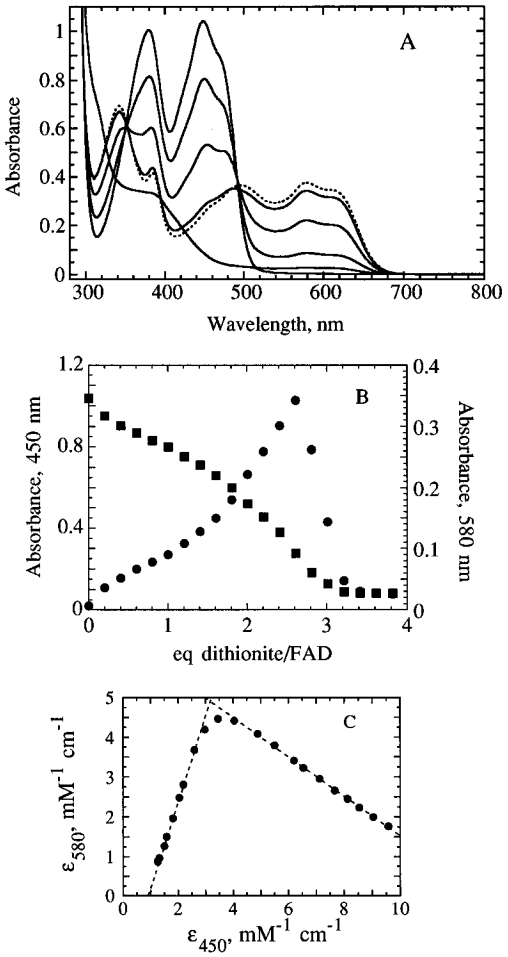

FIGURE 6: Anaerobic dithionite titration of AhpF. AhpF (65.5 nmol in 0.82 mL) was prepared and titrated as in the legend to Figure 5, except that no oxygen-scrubbing system was included, 0.66 nmol of methyl viologen was added, and aliquots of 20.3 mM dithionite were added from a titrating syringe. Panel A shows spectra obtained after addition of 0, 1.01, 2.01, 2.61, and 3.42 equiv of dithionite/FAD, in order of decreasing A_{450}. The calculated spectrum for the flavin semiquinone (dotted spectrum) was corrected for the presence of small amounts of oxidized and reduced flavin at maximal semiquinone formation. Panel B depicts the absorbance changes at 450 (squares) and 580 (circles) nm *vs* added dithionite. Panel C was generated from a separate experiment with more data points (a similar plot of the data from panels A and B was not significantly different). Values for extinction coefficients are plotted for 580 *vs* 450 nm. Lines were fit to points on each side of the three highest ϵ_{580} points and gave an ϵ_{580} of 4790 M^{-1} cm^{-1} and a value of 91% semiquinone at maximum formation.

Table 3: Extinction Coefficients of Different Redox Forms of AhpF

AhpF, redox form	342 nm	380 nm	385 nm	449 nm	500 nm	580 nm
oxidized	5460[a]	12620*	12230	13100*	2210	0
semiquinone, calcd[b]	8850*	4790	5050*	2830	4590*	4790*
reduced, calcd	4570	4180	4100*	1040	260	210

[a] Extinction coefficients are given in M^{-1} cm^{-1}. Asterisks denote values at absorbance maxima; others are shown for comparison. [b] Values for the semiquinone and reduced flavin spectra are given for the calculated spectra, as shown in Figure 6.

photoreduction; Zanetti et al., 1968), apparently reflecting a greater separation in reduction potentials between the single electron transfers $E(FAD) \rightarrow E(FADH^{\bullet})$ and $E(FADH^{\bullet}) \rightarrow E(FADH_2)$. All spectral changes above 500 nm seen during the dithionite titration are attributable to semiquinone forma-

tion. AhpF, like TrR, lacks the detectable charge transfer interaction between the nascent thiolate and oxidized flavin seen in other flavoprotein disulfide reductases (Williams, 1992).

Analyses of the stoichiometries of reductants required to elicit spectral changes indicate break points between phases at about 2.6−2.7 equiv/FAD. Oxidation of the pyridine nucleotide during NADH titrations can be monitored at about 350 nm, a wavelength where oxidized and semiquinone forms of the bound FAD are nearly isosbestic but NADH absorbs strongly (Figure 5B). At just over 5 electrons added per FAD (∼2.6 equiv of reductant/FAD), further NADH additions result in essentially no oxidation of the pyridine nucleotide, and semiquinone formation during dithionite titrations is maximal. In both cases, the two non-flavin centers have apparently accepted 2 electrons each, and 1-electron reduction to give the flavin semiquinone is at least partly complete. The final phase of semiquinone reduction during the dithionite titration is completed on addition of just over 3 equiv of dithionite/FAD, further confirming the presence of three redox centers per subunit in AhpF. Fully reduced AhpF is essentially completely reoxidized with 3 equiv of AhpC; spectral changes on addition of each aliquot of AhpC are the reverse of those seen during the dithionite reduction. The small amount of flavin semiquinone remaining after oxidation by AhpC (3−9%) is quickly reoxidized on exposure of the cuvette contents to air.

Spectral changes at 450 nm monitored over the course of NADH and dithionite titrations clearly indicate that, although all three redox centers of AhpF have similar reduction potentials (all three centers are partially reduced at each stage, giving rise to a complicated mixture of redox species), both redox-active disulfide centers are reduced preferentially relative to the FAD. This preferential reduction of the disulfides results in a changing slope for 450 and 580 nm absorbance changes, starting low and increasing in magnitude up to 2.6 equiv. The rise in A_{580} during dithionite titrations is more extensive than that with NADH. At 2 equiv of reductant added, reduction of the flavin cofactor is <40 and <63% complete for NADH and dithionite titrations, respectively, on the basis of the 450 nm values. Semiquinone formation at this stage (measured at 580 nm) is about 2-fold greater for dithionite titrations (∼58%) than for NADH titrations (∼29%).

As expected from the thiol titrations of NADH-reduced truncated and mutant AhpF proteins described earlier (Table 1), NADH titrations of C476,489A AhpF give very similar results compared with those of wild type. The truncated tryptic fragment of AhpF exhibits virtually identical spectral changes but consumes approximately 1 equiv less of NADH per FAD (data not shown).

A clear difference between spectral species generated during NADH and dithionite titrations is seen at long wavelengths (>700 nm); a small increase in long wavelength absorbance detected during the NADH titration is absent from dithionite titrations. At the point of full formation of this spectral species during NADH titrations (about 2.5−3 equiv/FAD), the flavin is predominantly in its semiquinone form (although not yet at maximum), with small amounts of both oxidized and reduced flavin, and the NADH has essentially all been oxidized to NAD^+. Identical final spectra can be obtained on titration of dithionite-reduced AhpF with NAD^+; nearly all of the NAD^+ is reduced concomitant with semiquinone formation, with an end point of about 0.6 equiv of NAD^+/FAD, and a long wavelength absorbance band is generated.

Our working hypothesis that this long wavelength absorbing species of AhpF could be attributed to $FADH_2 \rightarrow NAD^+$ charge transfer interaction was confirmed upon observation of spectral changes immediately following the addition of a 5-fold excess of NADH. A spectrum collected 12 s after addition showed a significantly reduced appearance of the flavin spectrum (>60% $FADH_2$) and a greatly enhanced long wavelength absorbance band (λ_{max} at approximately 730 nm). Progressive changes after this point indicated the formation of flavin semiquinone and loss of long wavelength absorbance over time. Intramolecular electron transfer to generate the semiquinone species is thus relatively slow and follows rapid oxidation of the NADH and formation of the long wavelength charge transfer species, consistent with our hypothesis. In contrast, dithionite titrations generate relatively high amounts of semiquinone-containing species first which decay to the equilibrium mixture of species over time. Redox species with $FADH_2 \rightarrow NAD^+$ interaction may be important as intermediates during catalytic turnover of AhpF, as has been suggested for the $FADH_2 \rightarrow NADP^+$ species of TrR (Prongay et al., 1989; Lennon & Williams, 1995; Williams, 1995).

DISCUSSION

The results described herein have led to the definitive identification of the two redox-active disulfide centers (Cys129−Cys132 and Cys345−Cys348) within the FAD-containing AhpF protein of AhpR. The two cysteine residues at the C-terminus (Figure 2) account for the two free thiols of oxidized AhpF and play no role in catalysis as assessed by site-directed mutagenesis. Although we have not yet begun to test the kinetic competence of redox forms of AhpF, there is strong reason to consider both disulfide redox centers in AhpF as important players in the overall peroxidatic mechanism. Loss of even DTNB reductase activity upon removal of the N-terminal region which includes the additional redox-active disulfide (relative to TrR) suggests that the N-terminus of AhpF is playing a very active role in catalysis and is not simply required for binding of AhpC.

The two intersubunit disulfide bonds of dimeric AhpC, which necessarily involve both Cys46 and Cys165, have also been shown to be reducible by NADH in the presence of AhpF and are fully reoxidized upon reaction with stoichiometric amounts of ethyl hydroperoxide. This evidence for a cysteine-based mechanism for the reduction of peroxides by *S. typhimurium* AhpC is entirely consistent with findings by Chae et al. (1994a) that the yeast TSA protein, a homologue of AhpC, requires the two analogous cysteinyl residues, Cys47 and Cys170, for catalysis of peroxide reduction. The most likely arrangement of these disulfide bonds in AhpC would be between Cys46 on one subunit and Cys165 on the other, so that two symmetrical active sites per dimer including residues from each subunit would be formed. Indeed, no evidence for asymmetry has been detected in reductive titrations shown here. Whatever the disulfide bond linkages, the redox-active disulfide centers of AhpC (and presumably its homologues) are, to our knowledge, unique in involving cysteine residues distant in the primary sequence (with 118 amino acids intervening).

Scheme 3

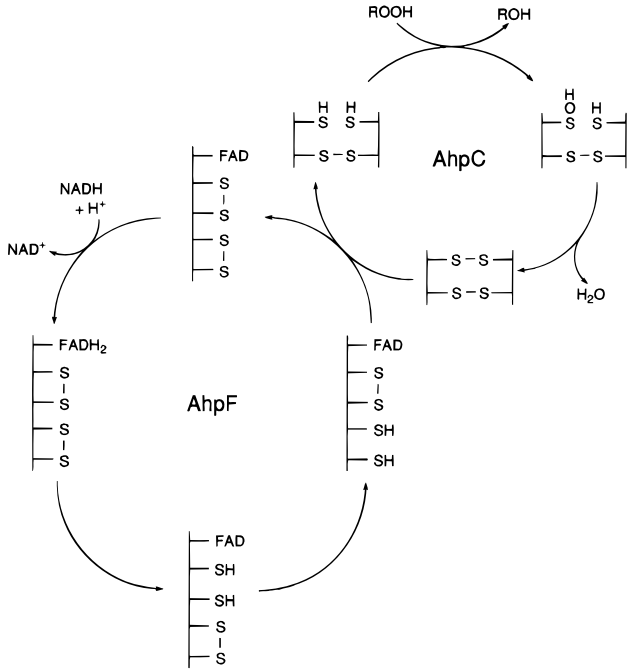

That the redox-active disulfide centers are apparently generated by bringing cysteinyl residues from different subunits together to form intersubunit bridges is even more striking.

In addition to identifying redox centers within AhpF and AhpC, we have shown that the full scheme of electron transfer from NADH to AhpF, AhpC and organic hydroperoxides is chemically feasible on the basis of static titrations. Redox centers appear to be appropriately poised for this electron transfer; disulfide centers within AhpF have similar, but higher, reduction potentials relative to the flavin.[2] Furthermore, electrons are transferred quantitatively from NADH to AhpC in the presence of a catalytic amount of AhpF, indicating that the reduction potentials of the redox-active disulfide centers of AhpC are higher and well-separated from that of NAD^+/NADH (−320 mV). The standard reduction potential of H_2O_2/H_2O is 1770 mV, a value which is undoubtedly far higher than those for the cystine disulfide centers of both proteins (Fasman, 1976). Accessibility of dithiol centers within reduced forms of AhpF and AhpC was demonstrated by rapid DTNB reaction with nondenatured, reduced AhpC and by the susceptibility of nascent thiols on each protein to inactivating modifications by thiol reagents (Poole & Ellis, 1996). This accessibility makes reasonable the suggestion that electrons can be directly transferred between AhpF and AhpC through thiol-disulfide interchange. Our proposal for the mechanism of electron transfer from reduced pyridine nucleotides to hydroperoxides is elaborated in Scheme 3.

The hypothesized path of electron transfer as depicted in Scheme 3 is supported by our results, reported within, and by a large body of work of others which has established much about the nature of enzymatic species generated during catalysis by the flavoprotein disulfide reductases (Williams, 1992). On the basis of the relationship between AhpF and TrR, we envision hydride transfer from reduced pyridine nucleotides to FAD, and electron transfer from the flavin to the Cys345−Cys348 disulfide center of AhpF, to occur essentially as it does in TrR. We suggest that intramolecular transfer of electrons to the Cys129−Cys132 center then follows, making thiol−disulfide interchange to the redox-active disulfide of AhpC possible. Our suggestion that one of the nascent cysteine thiols (Cys−SH) of AhpC is oxidized to a cysteine sulfenic acid (Cys−SOH) by the hydroperoxide substrate follows chemical precedent as established for this reaction during catalysis by the enterococcal flavoprotein NADH peroxidase (Poole & Claiborne, 1989b; Parsonage & Claiborne, 1995; Poole, 1994). Eukaryotic glutathione peroxidase has also been shown to catalyze H_2O_2 and alkyl hydroperoxide reduction through generation of an analogous oxidized residue, the selenenic acid form of the catalytic selenocysteine (Cys−SeOH; Epp et al., 1983). That disulfide bond formation would immediately follow this step in AhpC is likely given the presumed close proximity of the thiol group of the other cysteine residue in the active site (Claiborne et al., 1992). A similar mechanism has been proposed for peroxide reduction catalyzed by the thioredoxin-dependent peroxidase (formerly TSA) protein from *Saccharomyces cerevisiae* (Chae et al., 1994a).

As indicated, sequence searches and alignments have revealed that AhpF is a member of the TrR-like, pyridine nucleotide:disulfide oxidoreductase group of flavoproteins (Chae et al., 1994b; Kuriyan et al., 1991; Petsko, 1991; Tartaglia et al., 1990). Conservation of the known catalytic half-cystine residues of TrR (Cys135 and Cys138) is absolute among the homologues (Figure 1; Williams, 1992). TrR and AhpF branch apart from one another in the phylogenetic tree, however, due to an extended region of about 200 amino acids in AhpF and its close homologues which is absent from TrR-like proteins (Figures 1 and 2; Chae et al., 1994b). These bacterial flavoproteins more closely related to AhpF (top panel of Figure 1) have two conserved CXXC motifs, one of which is located within the N-terminus, and it is these four cysteinyl residues which have been identified in our work as redox centers in AhpF. As described in more detail below, the *Amphibacillus xylanus* flavoprotein identified as an NADH oxidase has also been shown to possess these reducible disulfide centers.

In the characterization of the redox properties of the recombinant *A. xylanus* NADH oxidase purified from *E. coli*, reductive titrations like those described herein for AhpF were performed with the *A. xylanus* flavoprotein (Ohnishi et al., 1994). There are many qualitative and quantitative similarities between the properties of these two flavoproteins, although several differences are notable. Like AhpF, the *A. xylanus* NADH oxidase possesses two redox-active disulfide centers which are reduced slightly preferentially relative to the flavin during the NADH titration. Blue, neutral flavin semiquinone and $FADH_2 \rightarrow NAD^+$ charge transfer species are also both seen. The extent of semiquinone formation is apparently considerably smaller (estimated at a maximum of 30% during dithionite titration on the basis of the extinction coefficient of the semiquinone species of TrR), although a significantly lowered extinction coefficient for this species might also account for some of the differences in titration results. Our calculated extinction coefficient at 580 nm for the AhpF semiquinone of about 4800 M^{-1} cm^{-1} (Table 3) is very similar to the value of 4600 M^{-1} cm^{-1}

[2] The complexity of reduced AhpF species given the three redox centers and the interdependence of reduction potentials of the three centers makes determinations of all values in the context of the redox state of the other centers very difficult.

reported for this species in TrR using similar methods (Zanetti et al., 1968).[3] As we have pointed out for AhpF, flavin semiquinone stabilized by the *A. xylanus* flavoprotein is also not likely to represent a catalytically relevant redox species. Like AhpF, the *A. xylanus* flavoprotein exhibits considerable long wavelength absorbance beyond 800 nm during the latter part of the NADH titration. Spectral changes may indicate a slightly greater propensity for NADH to fully reduce the flavin cofactor in the *A. xylanus* protein relative to that of AhpF.

Additional characterization of the redox centers of the *A. xylanus* NADH oxidase has been performed using mutant proteins lacking either or both cysteinyl residues (Cys337 and Cys340) which correspond to the catalytic residues of TrR (Ohnishi et al., 1995). All three mutants possess full NADH-dependent oxidase activity but are significantly impaired in their ability to reduce DTNB catalytically. Reductive titrations indicate the presence of only one redox center per subunit in all three mutants (the bound FAD). Although the CXXC motif within the N-terminus is still present in these mutants, it is no longer reducible without the intact Cys337−Cys340 redox center. These results, taken together with our own, indicate that the bound FAD within the intact or truncated (AhpF) protein is responsible for the H_2O_2-forming oxidase activity of the two flavoproteins, while both intact redox-active disulfide centers are also required (in addition to the flavin) for the disulfide reductase activity. Interestingly, it appears that the *A. xylanus* flavoprotein is more active as an oxidase (15 *vs* 1−2 s^{-1} without added FAD) and less active as a DTNB reductase (61.5 *vs* 275 min^{-1}) when compared with AhpF under similar conditions (Niimura et al., 1995; Ohnishi et al., 1994). Recent experiments carried out jointly between our two laboratories have now demonstrated that the *A. xylanus* NADH oxidase can, in fact, substitute for AhpF in catalysis of NADH-dependent cumene hydroperoxide and H_2O_2 reduction in the presence of *S. typhimurium* AhpC (Niimura et al., 1995). Identification of a partial open reading frame upstream of the structural gene for *A. xylanus* NADH oxidase as a homologue of AhpC (Chae et al., 1994b; Niimura et al., 1995) also strongly supports the conclusion that the *A. xylanus* flavoprotein is also part of an alkyl hydroperoxide reductase system in these Gram-positive bacteria.

We have given a great deal of consideration to the extent to which AhpF and TrR may behave similarly, yet in a different context. Efforts to produce a model of the three-dimensional structure of the C-terminal portion of AhpF based on the TrR structure have indicated a reasonable fit between the two structures in most regions (J. D. Schmitt and L. B. Poole, unpublished observations). One of the most notable differences between AhpF and TrR is the additional redox-active disulfide center which appears to mediate electron transfer between Cys345−Cys348 of AhpF and the 42 kDa AhpC dimer. It has been postulated that TrR undergoes major conformational changes as it shifts the redox-active dithiol from interaction with the flavin (consistent with the crystal structure) to interaction with the 11.8 kDa protein thioredoxin (hypothesized structure; Waksman et al., 1994). A similar argument is possible for AhpF, where, in addition to the two redox centers which must alternate interactions, a third center (Cys129−Cys132) must presumably flip between interaction with the dithiol form of Cys345−Cys348, and interaction with the large AhpC substrate. A reasonable working model for these interactions is depicted in Scheme 4.

Scheme 4

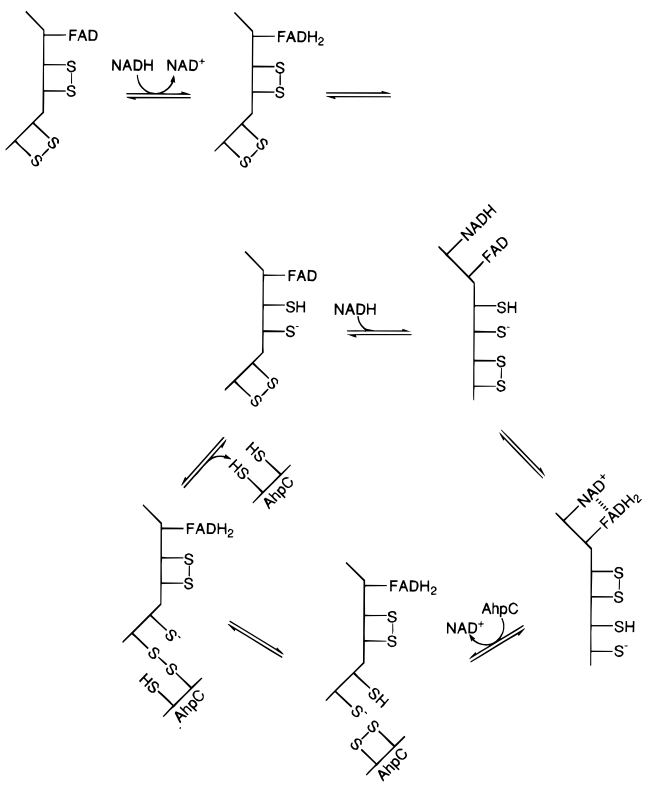

As perhaps follows from the preceding discussion, we have come to regard AhpF as a TrR-like protein with a "tethered" redox-active domain analogous to Tr. The N-terminal domain of AhpF is significantly larger than Tr (∼208 *vs* 109 amino acids for Tr) but contains a redox-active CXXC motif, like Tr or perhaps glutaredoxin, which apparently shunts electrons between the donor and several acceptors. Other observations support this view, as well. *E. coli* TrR, in the presence of Tr but not in its absence, can replace AhpF in catalyzing turnover with AhpC, ethyl hydroperoxide, and NADPH (L. B. Poole, unpublished observations). TrR plus Tr have also recently been identified as the reductase system linked to peroxidase function of AhpC homologues from *S. cerevisiae* (Chae et al., 1994a) and *Entamoeba histolytica* (L. B. Poole, H.-Z. Chae, B. M. Flores, S. G. Rhee, D. L. Diedrich, and B. E. Torian, manuscript submitted). Furthermore, although most bacterial homologues to the *S. typhimurium* AhpR system have an identical arrangement of open reading frames corresponding to *ahpC* and full-length *ahpF*, *Clostridium pasteurianum* gene organization is quite different and appears to include genes encoding a smaller (TrR-like) flavoprotein, a glutaredoxin-like protein, and an AhpC homologue (Figure 7; Mathieu & Meyer, 1993; Mathieu et al., 1992). Thus, in the one case where the structural gene related to *ahpC* is oriented downstream of an *ahpF* homologue (truncated), an additional open reading frame appears to encode an additional redox protein. In a

[3] Later work by O'Donnell and Williams (1983) revised this value to 3400 M^{-1} cm^{-1}, taking into account the two semiquinone spectral species seen in the presence of the disulfide or dithiol form of the second redox center.

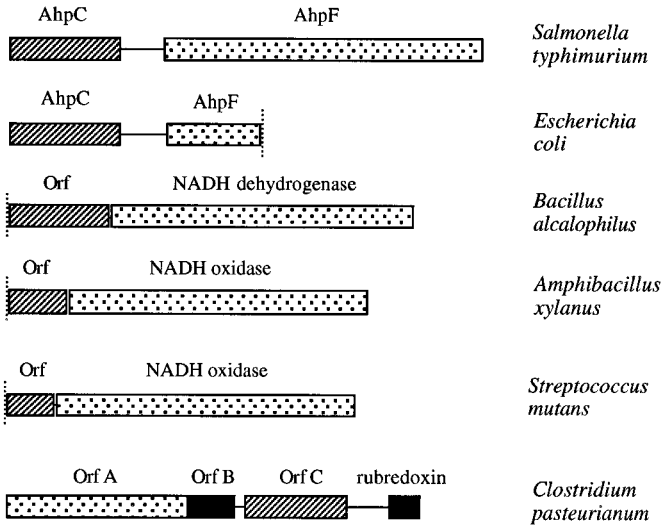

FIGURE 7: Organization of structural genes of AhpR homologues from different bacterial sources. AhpC homologues are depicted with hatched bars and AhpF homologues with stippled regions. Intergenic regions are shown as lines, and black areas indicate other redox proteins encoded on a genomic clone from *C. pasteurianum* (a glutaredoxin-like protein encoded by Orf B and rubredoxin; Mathieu & Meyer, 1993; Mathieu et al., 1992). Partially deduced sequences are indicated by broken lines at one end, and Orf designations refer to open reading frames which were not originally identified as known structural genes. Coding and noncoding regions are drawn to scale.

recent finding of great import to this discussion, TrR and Tr genes, normally found widely separated on the bacterial chromosome in many species, were found not only in close proximity in some species of mycobacterium but also as a fused hybrid gene which apparently encodes a bifunctional protein in *Mycobacterium leprae* (Wieles et al., 1995). A striking difference between this TrR/Tr hybrid of *M. leprae* and the AhpF homologues from a number of different bacteria is the location of the Tr-like region C-terminal to the TrR. Clearly, many overlapping functions of a number of different redox proteins combine in a variety of ways to protect living organisms against oxidant-linked damage.

ACKNOWLEDGMENT

The author thanks Lois LaPrade for technical help, Charles H. Williams, Jr., for his gift of *E. coli* thioredoxin reductase, and Gisela Storz and Al Claiborne for valuable discussions.

REFERENCES

Bull, C., & Ballou, D. P. (1981) *J. Biol. Chem. 256*, 12673−12680.
Chae, H. Z., Chung, S. J., & Rhee, S. G. (1994a) *J. Biol. Chem. 269*, 27670−27678.
Chae, H. Z., Robison, K., Poole, L. B., Church, G., Storz, G., & Rhee, S. G. (1994b) *Proc. Natl. Acad. Sci. U.S.A. 91*, 7017−7021.
Claiborne, A., Ross, R. P., & Parsonage, D. (1992) *Trends Biochem. Sci. 17*, 183−186.
Epp, O., Ladenstein, R., & Wendel, A. (1983) *Eur. J. Biochem. 133*, 51−69.
Fasman, G. D. (1976) *Handbook of Biochemistry and Molecular Biology, Physical and Chemical Data*, 3rd ed., CRC Press, Inc., Boca Raton, FL.
Flohé, L., Loschen, G., Günzler, W. A., & Eichele, E. (1972) *Hoppe-Seyler's Z. Physiol. Chem. 353*, 987−999.
Fullmer, C. S. (1984) *Anal. Biochem. 142*, 336−339.
Jacobson, F. S., Morgan, R. W., Christman, M. F., & Ames, B. N. (1989) *J. Biol. Chem. 264*, 1488−1496.
Kuriyan, J., Krishna, T. S. R., Wong, L., Guenther, B., Pahler, A., Williams, C. H., Jr., & Model, P. (1991) *Nature 352*, 172−174.
Lennon, B. W., & Williams, C. H., Jr. (1995) *Biochemistry 34*, 3670−3677.
Massey, B., & Palmer, G. (1966) *Biochemistry 5*, 3181−3189.
Mathieu, I., & Meyer, J. (1993) *FEMS Microbiol. Lett. 112*, 223−228.
Mathieu, I., Meyer, J., & Moulis, J. M. (1992) *Biochem. J. 285*, 255−262.
Niimura, Y., Poole, L. B., & Massey, V. (1995) *J. Biol. Chem. 269* (in press).
O'Donnell, M. E., & Williams, C. H., Jr. (1983) *J. Biol. Chem. 258*, 13795−13805.
Ohnishi, K., Niimura, Y., Yokoyama, K., Hidaka, M., Masaki, H., Uchimura, T., Suzuki, H., Uozumi, T., Kozaki, M., Komagata, K., & Nishino, T. (1994) *J. Biol. Chem. 269*, 31418−31423.
Ohnishi, K., Niimura, Y., Hidaka, M., Masaki, H., Suzuki, H., Uozumi, T., & Nishino, T. (1995) *J. Biol. Chem. 270*, 5812−5817.
Parsonage, D., & Claiborne, A. (1995) *Biochemistry 34*, 435−441.
Petsko, G. A. (1991) *Nature 352*, 104−105.
Poole, L. B. (1994) in *Flavins and Flavoproteins 1993* (Yagi, K., Ed.) pp 583−586, Walter de Gruyter & Co., New York.
Poole, L. B., & Claiborne, A. (1989a) *J. Biol. Chem. 264*, 12322−12329.
Poole, L. B., & Claiborne, A. (1989b) *J. Biol. Chem. 264*, 12330−12338.
Poole, L. B., & Ellis, H. R. (1996) *Biochemistry 35*, 56−64.
Prongay, A. J., & Williams, C. H., Jr. (1992) *J. Biol. Chem. 267*, 25181−25188.
Prongay, A. J., Engelke, D. R., & Williams, C. H., Jr. (1989) *J. Biol. Chem. 264*, 2656−2664.
Riddles, P. W., Blakeley, R. L., & Zerner, B. (1979) *Anal. Biochem. 94*, 75−81.
Russel, M., Kidd, S., & Kelley, M. R. (1986) *Gene 45*, 333−338.
Storz, G., Jacobson, F. S., Tartaglia, L. A., Morgan, R. W., Silveira, L. A., & Ames, B. N. (1989) *J. Bacteriol. 171*, 2049−2055.
Tartaglia, L. A., Storz, G., Brodsky, M. H., Lai, A., & Ames, B. N. (1990) *J. Biol. Chem. 265*, 10535−10540.
Thannhauser, T. W., Konishi, Y., & Scheraga, H. A. (1984) *Anal. Biochem. 138*, 181−188.
Waksman, G., Krishna, T. S. R., Williams, C. H., Jr., & Kuriyan, J. (1994) *J. Mol. Biol. 236*, 800−816.
Wieles, B., van Soolingen, D., Holmgren, A., Offringa, R., Ottenhoff, T., & Thole, J. (1995) *Mol. Microbiol. 16*, 921−929.
Williams, C. H., Jr. (1992) in *Chemistry and Biochemistry of Flavoenzymes* (Müller, F., Ed.) pp 121−211, CRC Press, Inc., Boca Raton, FL.
Williams, C. H., Jr. (1995) *FASEB J. 9*, 1267−1276.
Zanetti, G., Williams, C. H., Jr., & Massey, V. (1968) *J. Biol. Chem. 243*, 4013−4019.

BI951888K